



# Silica Aerogel/Potassium Hexatitanate Whisker Composite Coated Fabric for Metallurgical Protective Clothing

Jie Wang<sup>1,2</sup> · Mengling Wang<sup>1,2</sup> · Liuxiang Zhan<sup>1,2</sup> · Ni Wang<sup>1,2</sup>

Received: 26 April 2022 / Revised: 16 July 2022 / Accepted: 31 August 2022 / Published online: 15 February 2023  
© The Author(s), under exclusive licence to the Korean Fiber Society 2023

## Abstract

Silica aerogel/potassium hexatitanate whisker composite coated fabric was successfully prepared by polyacrylate coating, which could further improve the thermal insulation property of the fabric and provide more efficient thermal protection. The results show that with the increase of the proportion of aerogel particles, the thermal insulation property of the coated fabric first increases and then decreases. When the mass ratio of silica aerogel particles to potassium hexatitanate whisker is 3:7, the composite coated fabric has the best thermal insulation performance with thermal conductivity of 0.232 W/(m·k). After the heat source irradiated the fabric, the temperature difference of the inner and outer of the coated fabric decreased by 16.1 °C and 19.35 °C, respectively, compared with the original fabric, and the composite coated fabric exhibited more than 75% reflectivity in the near-infrared band. Also, in the test of resistance of the coated fabric to molten metal splash, after the coated fabric was poured with 250 g of molten aluminum, the surface of the coated fabric was not adhered by molten aluminum, and the coated fabric was not burned through and remained intact in appearance, and the PVC film attached to the back of the coated fabric was not damaged, the surface texture of PVC film was clear, indicating that the composite coated fabric has a good thermal protection effect.

**Keywords** Silica aerogel · Potassium hexatitanate whisker · Coated fabric · Thermal insulation property · Molten metal splashes

## 1 Introduction

Traditional metal droplet protective fabrics for metallurgy, electric welding, and other industries are usually thickened cotton fabric with flame-retardant treatment and aluminum-coated fabrics. However, the temperature is as high as thousands of degrees Celsius and accompanied by a large amount of infrared radiation when many metals are melted, once they come into contact with the fabric, the surface structure of the fabric will be ablated, and then the molten metal will adhere to the surface of the fabric and rapidly releasing heat, which will burn through the fabric and cause burns and scalds for operators [1–4]. Therefore, the development

of lightweight and efficient thermal insulation fabrics has become the research focus of metallurgical protective clothing due to the limited protective effect of traditional protective clothing, which is also too heavy for workers to escape in emergencies [5].

The enterprises that can develop and produce molten metal splash protective fabric are mainly located in Europe, America, and other developed countries and regions, such as GENTEX, DuPont, and LERNARD. The related research focused on the fabrics with fiber blends containing both flame-retardant natural fibers and inherently flame-retardant synthetic fibers, and protective fabric with different quality and targeted protection according to the characteristics of different metals, but such products are not only expensive but also difficult to popularize [1]. The research of molten metal splash protection products in China is in the initial stage, the main product is the heavy cotton fabrics with flame-retardant finished and blended fabric made of wool and other flame-retardant fibers, which will fracture the molten metal to achieve a protective effect by the elasticity of the scales on the surface of wool fiber; although this

✉ Ni Wang  
wangni@dhu.edu.cn

<sup>1</sup> Key Laboratory of Textile Science and Technology of Ministry of Education, College of Textiles, Donghua University, Shanghai 201620, China

<sup>2</sup> Engineering Research Center of Technical Textiles, Ministry of Education, Donghua University, Shanghai 201620, China

type of product has a certain protective effect, it has poor high-temperature resistance, and the fabrics that use lots of wool have obvious itchiness when worn and have poor shape retention, so they have not been widely used [6]. It is significant to study durable protective fabric that can not only be flame retardant and high temperature resistant but also prevent molten metal splashing.

Silica aerogel is a low thermal conductivity material with high porosity and low density formed by nanometric particles, its three-dimensional skeleton structure, which greatly increases the thermal transfer path in the solid skeleton, makes the thermal conductivity reduce evidently, so it has been broadly applied in thermal protection [7–10]. Because block silica aerogel has the disadvantages of brittle texture, easy breaking, insufficient filling, and low utilization efficiency, so the application of granular aerogel has a greater prospect of development. However, with the increasing temperature, heat radiation has become the main way of thermal conduction, and infrared radiation of 3 to 8  $\mu\text{m}$  can easily pass-through silica aerogel. So, if some functional particles, which can scatter or reflect the infrared radiation, are introduced into the silica aerogel, the thermal transfer by radiation will be reduced and its thermal insulation properties will be improved [11–13]. For example, Wei et al. [14] developed a facile one-step polymer-incorporation sol–gel process, together with a surface modification and an ambient pressure drying processes, to prepare silica-PVP composite aerogels, which were characterized to possess good mechanical strength (Young's modulus of bending > 30 MPa) and lower high-temperature thermal conductivity (0.063 W/m·k at 300 °C); Zeng et al. [15] used carbon black as a opacifier to explore the effect of the content of the opacifier on the thermal conductivity of silica aerogels from a theoretical level, which calculated the extinction coefficient of carbon black particles by using Rayleigh scattering theory; Yao et al. [16] reported the preparation of the aluminum-doped silica aerogel (ASA) by the sol–gel and ambient pressure drying method using cheap industrial water glass as the silicon source and aluminum chloride as the aluminum source, respectively, which found that the incorporation of Al atoms could effectively improve the heat resistance of silica aerogels, and the sample with Al/Si molar ratio of 0.15 showed the best heat insulation performance. Yuan et al. [11] fabricated a silica aerogel composite by adding  $\text{TiO}_2$  particles and glass fibers and found the increasing of glass fibers favored the improvement of the strength and thermal insulation conductivity of the composites, and  $\text{TiO}_2$  could decrease the thermal conductivity abruptly at high temperatures, and the forming pressure of 1.5 MPa was optimal for the heat insulation property.

Potassium hexatitanate whiskers ( $\text{K}_2\text{O}\cdot 6\text{TiO}_2$ , PTW) possess many advantages such as low cost, environment-friendly, excellent chemical stability, good mechanical

properties, high thermal insulating ability and high infrared reflectivity, which can withstand the high temperature of 1200 °C, its thermal conductivity at room temperature is as low as 0.089 W/(m·k) and has a negative thermal conductivity (the thermal conductivity decreases with the increase of temperature), so the thermal conductivity is only 0.017 W/(m·k) at 800 °C. In addition, there is a good composite effect between potassium hexatitanate whiskers and polymers, which results in an easy process and wide applications [17–19].

Polyacrylate is an aqueous polymeric adhesive made by emulsion copolymerization of acrylate monomers. Due to its low price, simple preparation process, good mechanical strength and weather resistance, polyacrylate is one of the most widely used polymer materials, which can be used in coatings, textile printing and dyeing, etc., and can be applied as functional materials in many other fields [20, 21]. The advantages of using polyacrylate as a coating agent are good film formation, light transmission, high elasticity, biodegradability, acid and alkali resistance, chemical resistance and aging resistance. Thermal insulating particles can be firmly bonded to the surface of the fabric by the bonding action of polyacrylate and thus can perform their thermal insulation properties to protect the fabric in case of high temperature.

In this work, silica aerogel powder was used as heat insulating particles, and potassium hexatitanate whisker was used as an opacifier, then silica aerogel/potassium hexatitanate whisker composite coated fabric for metallurgical protective clothing was prepared by polyacrylate coating, and the effect of the ratio between silica aerogel and potassium hexatitanate whisker on thermal insulation property of the composite coated fabric was discussed.

## 2 Experimental

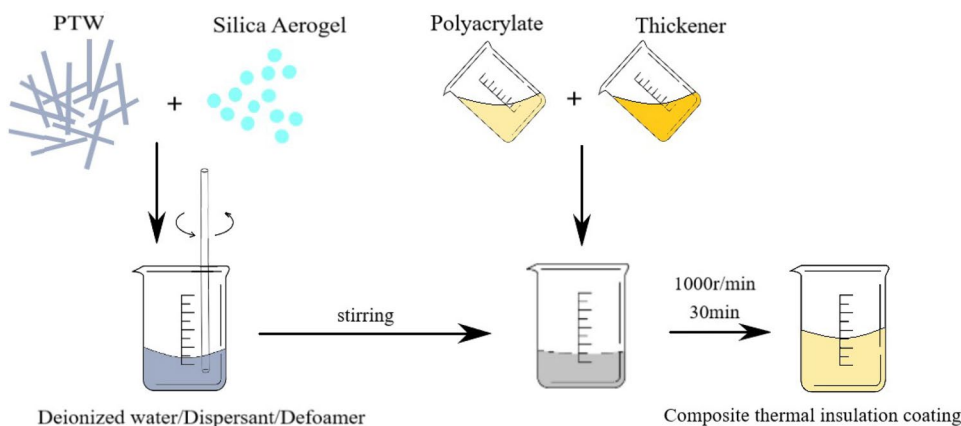
### 2.1 Materials

Flame-retardant fabric (combed cotton/high strength nylon/Tencel, 271.5 g/m<sup>2</sup>) was provided by Shandong Woyuan New Fabric Co., Ltd. Silica aerogel powder was purchased from IBIH New Materials Co., Ltd. PTW was purchased from Shandong Dongying Xinyi Chemical Co., Ltd. Polyacrylate emulsion purchased from Shanghai Baolijia Chemical Co., Ltd. Dispersants, defoamers, and thickeners were provided by Shanghai Yipin Textile Technology Co., Ltd. Deionized water was used in all experiments.

### 2.2 Preparation of Composite Thermal Insulation Coating Agent

The preparation of the composite thermal insulation coating agent is illustrated in Fig. 1. As shown below, an appropriate

**Fig. 1** Preparation of composite thermal insulation coating agent



amount of dispersant and defoamer was firstly added into deionized water and stirred with a glass rod. Then, silica aerogel powder, PTW, and polyacrylate emulsion were added to the system in turn while stirring, followed by an appropriate amount of thickener. Finally, the obtained mixture was stirred at 1000 r/min for 30 min to obtain a silica aerogel/potassium hexatitanate whisker composite coating agent, which was left 30 min for use.

In the above composite coating agent, the mass ratio of deionized water and polyacrylate emulsion was 8:2, the mass of dispersant accounted for 1.5% of the total mass of particles, the mass of defoamer accounted for 1% of the mass of deionized water, and the mass of thickener accounted for 0.8% of the total mass of the composite coating agent, the calculation formula of the total particle content in the coating agent was as follows:

$$\text{Particle content, \%} = \frac{C_0 + C_3}{C_1 + C_2} \times 100\% = 15\% \quad (1)$$

where  $C_0$  was the mass of aerogel powder;  $C_1$  was the mass of deionized water;  $C_2$  was the mass of polyacrylate emulsion;  $C_3$  was the mass of PTW, and  $C_1:C_2$  was 8:2. Based on the total particle content of 15%, the composite coated fabric was prepared and the mass ratio of silica aerogel particles and PTW were 1:9, 2:8, 3:7, 4:6, and 5:5, respectively. For example, for a composite coated fabric with a particle ratio of 1:9, the mass of deionized water and polyacrylate emulsion in the coating agent was 80 g and 20 g, respectively; and the mass of silica aerogel and potassium hexatitanate whisker was 1.5 g and 13.5 g, respectively. That was, the total mass of the silica aerogel and the potassium hexatitanate whisker

accounted for 15% of the total mass of the deionized water and the polyacrylate emulsion. In addition, 7.5% silica aerogel-coated fabric was also prepared (the ratio of silica aerogel to PTW was 5:0).

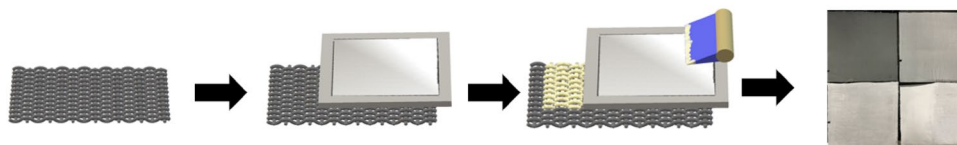
### 2.3 Preparation of Composite Coated Fabrics

As shown in Fig. 2, a screen printing plate was employed to evenly coat the prepared thermal insulation coating agent on the surface of the original fabric. Firstly, a screen printing plate was placed on the surface of the original fabric and then dipped an appropriate amount of thermal insulation coating agent with a scraper, the position of the screen printing plate and the fabric remained unchanged, and then, the scraper was used to repeatedly scrape and coat the surface of the screen printing plate (3~4 times), the coating agent could cover the surface of the fabric through the pores of the screen printing plate, when the coating agent was scraped evenly and then the fabric was taken out for drying. The specific process was: the original fabric was scraped and coated (2~4 times) → dried (100°C × 3 min) → secondary scraped and coated (2~4 times) → dried (100°C × 3 min) → baked (150°C × 2 min) → composite coated fabric.

### 2.4 Characterization

SEM (DXS-10ACKT, Japan) was employed to observe the micromorphology of coated fabrics and PTW. The crystal structure of particles on the surface of coated fabric was characterized by using an X-ray polycrystalline diffractometer (Bruker D8, Germany) with a diffraction intensity collection range of 0~90° and a power of 2.2 kW. Fourier transform

**Fig. 2** The schematic diagram of the coating process



infrared microscopic imaging spectrometer (Nicolet-6700, America) was employed to measure the infrared transmittance of the coated fabrics through ATR (attenuated total reflection) method. The UV–Vis–NIR reflectivity was measured by using a UV–Vis–NIR spectrophotometer (UV-3600, Japan) with a scanning wavelength of 250~2500 nm, and a scanning speed of high speed. The thermal conductivity of coated fabric was determined by using a multifunctional rapid thermal conductivity tester (DRE-III, China) with the thermal power of 0.5 W, the test time of 40 s, and the sampling interval of 200 ms, and the background material of quartz glass. As shown in Fig. 3, the self-made device was adopted to test the temperature change of the back of the fabric under the heat source, the fabric can be placed in the opening and exposed to the heat source, and then the temperature rise of the back of the fabric was tested after 360 s. And the infrared thermal imager (Fluke TIS75, America) was also employed to test the surface temperature of the fabric. The molten metal splash tester for protective clothing (Sutong, China) was used to test the anti-molten metal aluminum impact performance of fabric according to ISO 9185:2007.

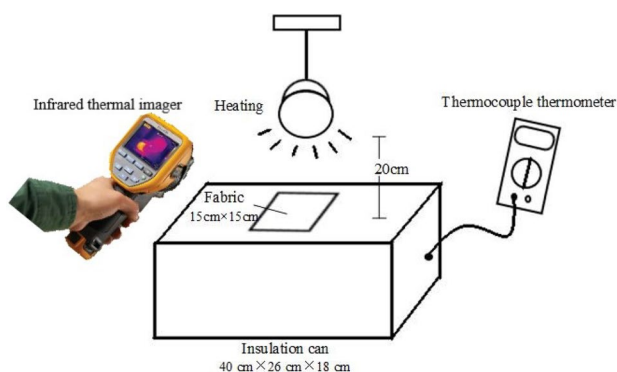


**Fig. 3** A simple device for testing the temperature change of coated fabrics under the heat source

### 3 Results and Discussion

#### 3.1 Surface Morphology Investigation of Coated Fabric

As shown in Fig. 4a, the appearance of PTW was cylindrical form with a large aspect ratio, the length of a single whisker was about 15–25  $\mu\text{m}$ , and the diameter was about 1  $\mu\text{m}$ . From Fig. 4b, it could be found that both the PTW and silica aerogel particles were evenly distributed and bonded to the surface of the fabric after coating. With the content of silica aerogel in the composite coated fabric increased, as shown in Fig. 4c, when the content of silica aerogel in the composite coated fabric was too high, it could be observed that many block solids with large volumes and irregular shapes appeared on the surface of the fabric. These solids were formed by the mutual agglomeration of PTW and silica aerogel, which also had a large mass as well as were not wrapped in the polyacrylate, so had a high probability of falling off from the surface of the coated fabric. The agglomeration phenomenon and the number of block solids were proportional to the content of silica aerogel particles. This was mainly because the hydrophobicity of silica aerogel particles was very strong so had the poor dispersion in water-based coating agent, so the aerogel particles in water-based coating agent would agglomerate due to their large surface energy and the van der Waals force between the particles and would adsorb the PTW in the coating agent in the agglomeration process.

#### 3.2 Crystal Analysis of the Surface of Coated Fabrics

As shown in Fig. 5, the XRD patterns of the various composite coated fabrics were examined to gain more insight into the crystal types of the thermal insulation particles on the surface of the composite coated fabrics. The obvious peaks corresponding to the presence of PTW compositions

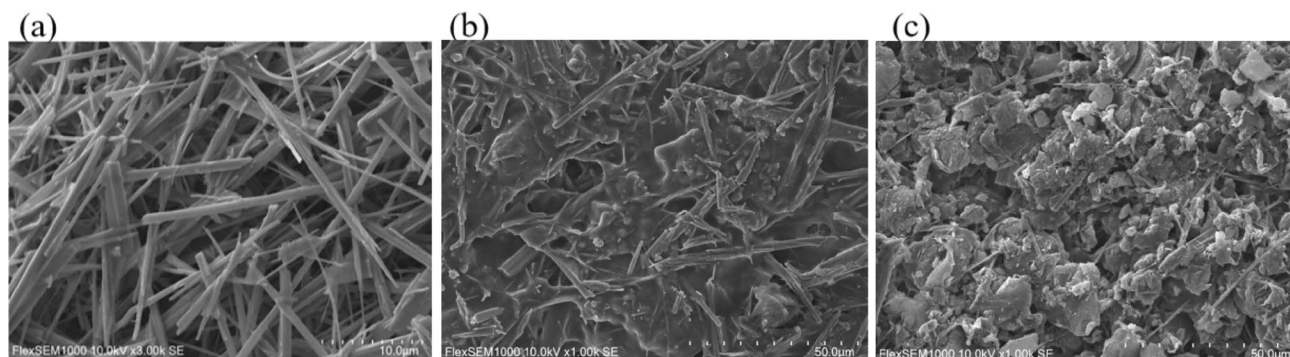


**Fig. 4** SEM images of **a** PTW and **b–c** Silica aerogel/PTW composite coated fabrics with the mass ratio of aerogel to PTW were 1:9 and 5:5, respectively



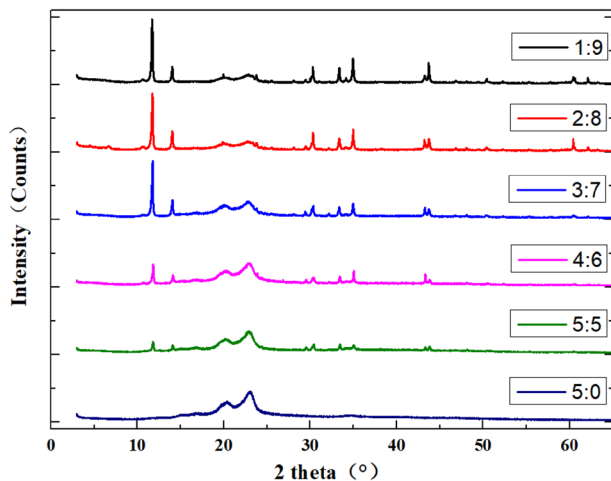


Fig. 5 XRD patterns of the various composite coated fabrics

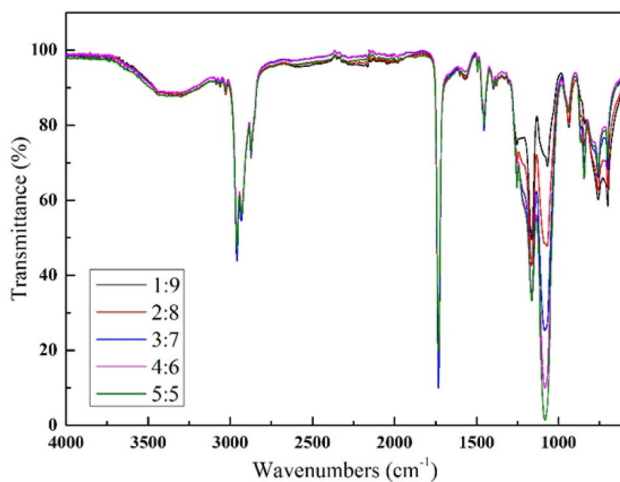


Fig. 6 FT-IR spectra of the various composite coated fabrics

on silica aerogel/PTW composite coated fabrics were seen, which confirmed the presence of PTW particles on the coated fabrics. The intensity of the peak correlates with the concentration of PTW particles in composite coating. The strong and sharp peaks indicate the crystalline nature of the PTW particles in the composite coating [22]. However, there was no obvious characteristic crystalline diffraction peak about silica aerogel in the XRD pattern, only the diffraction peak of the amorphous structure appears when  $2\theta$  was about  $23^\circ$ , and the intensity was small, indicating that the silica aerogel particles in the composite coating were amorphous.

### 3.3 FT-IR Spectra of Coated Fabrics

The FT-IR spectra of composite coated fabrics with different particle ratios at  $600\sim 4000\text{ cm}^{-1}$  are shown in Fig. 6, where the absorption peak at  $3353\text{ cm}^{-1}$  corresponded to

the antisymmetric stretching vibration of -OH in adsorbed water, and the peaks near  $2958\text{ cm}^{-1}$  represented the stretching vibration of -CH and -CH<sub>2</sub>, respectively, indicating that SiO<sub>2</sub> aerogel contained a small amount of unhydrolyzed Si-O-C<sub>2</sub>H<sub>5</sub>. And the absorption peak of the stretching vibration of the Si-OH group at  $939\text{ cm}^{-1}$ . The absorption peaks at  $1085\text{ cm}^{-1}$  and  $768\text{ cm}^{-1}$  corresponded to the antisymmetric and symmetric stretching vibrations of Si-O-Si in aerogels, respectively. As can be seen from Fig. 6, the introduction of a small amount of PTW did not damage the structure and composition of the silica aerogel itself, and the structure and composition of the silica aerogel did not change significantly with the increase of the doping amount.

### 3.4 Thermal Conductivity of Coated Fabrics

Under normal temperature conditions, the thermal conductivity of silica aerogel particles was much smaller than that of PTW. After the two kinds of particles were coated on the surface of the fabric as combined fillers, the aerogel particles with lower thermal conductivity played a dominant role. The silica aerogel particle had a high porosity of 99% and a spatial grid structure, and a large amount of static air with low thermal conductivity was stored inside its particles. Therefore, after coating the silica aerogel particle onto the surface of the fabric, a layer of air with low thermal conductivity could be constructed on the surface of the coated fabric, thus delaying the heat conduction in the structure of the coated fabric and reducing the thermal conductivity of the coated fabric. However, this did not mean that the higher the content of silica aerogel particle, the lower the thermal conductivity of the composite coated fabric. The silica aerogel particles in the coating agent would gather together due to the van der Waals force and large surface energy, but when the content of particles was low, the distance between the particles in the coating agent was farther, and the van der Waals force was weaker, so the possibility of inter-particle agglomeration was low, once the content of particles exceeded a certain value, then inter-particle agglomeration would occur in large quantities, and this agglomeration behavior would make the particles lose their original function and weaken the thermal protection performance of the coating agent and the coated fabric, which was manifested as the coating agent became very viscous, dry and hard, and did not have mobility, and when the above coating agent was coated to the surface of the fabric, there will be obvious small solids on the surface of the coated fabric. As shown in Fig. 7, with the increase of the aerogel particles, the thermal conductivity of the coated fabric first decreased and then increased gradually. When the ratio of aerogel to PTW was 3:7 in the composite coating, the thermal conductivity of the

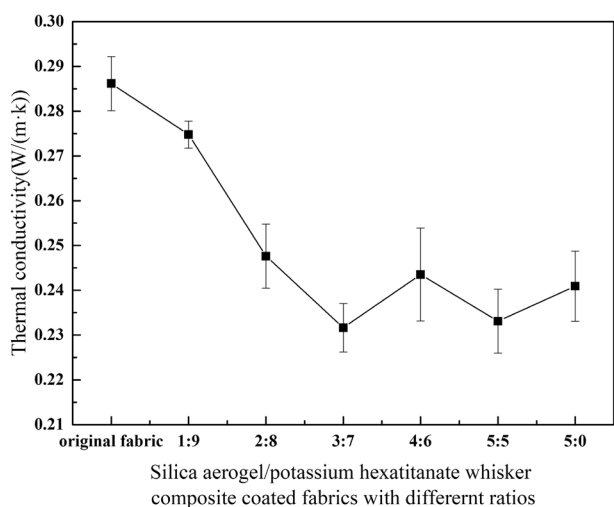


**Fig. 7** Thermal conductivity of various composite coated fabrics

coated fabric was the lowest, which was 19% lower than that of the original fabric, and 3.84% lower than that of the aerogel-coated fabric with a particle ratio of 5:0, indicated that adding an appropriate proportion of PTW had a positive effect for further reducing the thermal conductivity of coated fabric, this was because PTW had a low thermal conductivity and stable chemical property, so added the right amount of PTW could increase the total number of thermal insulation particles on the surface of the composite coated fabric and further reduced the heat transfer. When the content of silica aerogel in the composite coated fabric continued to increase, the thermal conductivity of the composite coated fabric reversed and began to rise, which might be due to the existence of large van der Waals forces between the excess silica aerogel particles and large surface energy of silica aerogel so agglomeration occurred, made a large number of particles gathered together to form a larger volume of solid material, this agglomeration behavior tended to weaken the properties of the individual particles, so the thermal conductivity of the solid material formed by agglomeration was usually higher than that of the individual particles. Moreover, these solids had a larger volume and mass compared to individual particles and therefore had a higher probability of falling off from the surface of the coated fabric after coating, which will further weaken the thermal insulation property of the composite coated fabric once the particles fall off. Therefore, when the ratio of silica aerogel to PTW was 3:7, the thermal conductivity of the composite coated fabric was the lowest. If the content of silica aerogel particles in the composite coating continued to increase, it would not further reduce the thermal conductivity of the composite coated fabric

due to the agglomeration that would occur between the particles.

### 3.5 Thermal Insulation Performance of Coated Fabrics

As shown in Fig. 3, the thermocouple thermometer was employed to detect the temperature of the back of the coated fabric under the heat source, and the infrared thermal imager was used to directly display the surface temperature of the coated fabric under the heat source.

As shown in Fig. 8 a~d, after being irradiated by a heat source, the surface temperature of the composite coated fabric with PTW added was significantly lower than that of the original fabric and the aerogel-coated fabric, indicating that the doping PTW could further enhance the thermal insulation performance of the coated fabric. When the ratio of silica aerogel and PTW was 3:7, the surface temperature of the composite coated fabric was the lowest which decreased by 19.35 °C and 7.6 °C, respectively, compared with that of the original fabric and aerogel-coated fabric. This may be because there were more functional particles in the composite coating that could block heat after the addition of PTW, and PTW has high infrared reflection property, which could isolate and reflect the near-infrared light with high energy, so when the light that contained high heat irradiated the surface of the coated fabric, PTW in the composite coating could reflect part of the heat first, to avoid all the heat accumulate on the surface of the coated fabric, and the thermal insulation coating formed by the low thermal conductivity of silica aerogel and PTW together on the surface of the fabric could also isolate or reduce the heat transfer from the external environment to the fabric structure as much as possible, thus reduced thermal damage.

The temperature rise of the back of the fabric is shown in Fig. 8e after the fabric was irradiated by a heat source. The temperature rise rate of each fabric was the fastest within 0~120 s and gradually became flat after 120 s, among them the temperature rise rate of the original fabric was the fastest, which the final temperature at 360 s exceeding 90 °C. The temperature rise rate of fabric after coating was significantly lower than that of the original fabric, and when the mass ratio of silica aerogel particles and PTW was 3:7, the temperature rise rate and final temperature of the composite coated fabric was the lowest and lower than that of the aerogel-coated fabric with a mass ratio of 5:0, indicating that the combination of the two thermal insulation particles could further improve the thermal insulation performance of the coated fabric. When the content of silica aerogel in the composite coated fabric continued to increase, the thermal insulation property of the composite coated fabric began to decline, and its surface temperature and temperature rise rate increased, which was due to the agglomeration that occurred

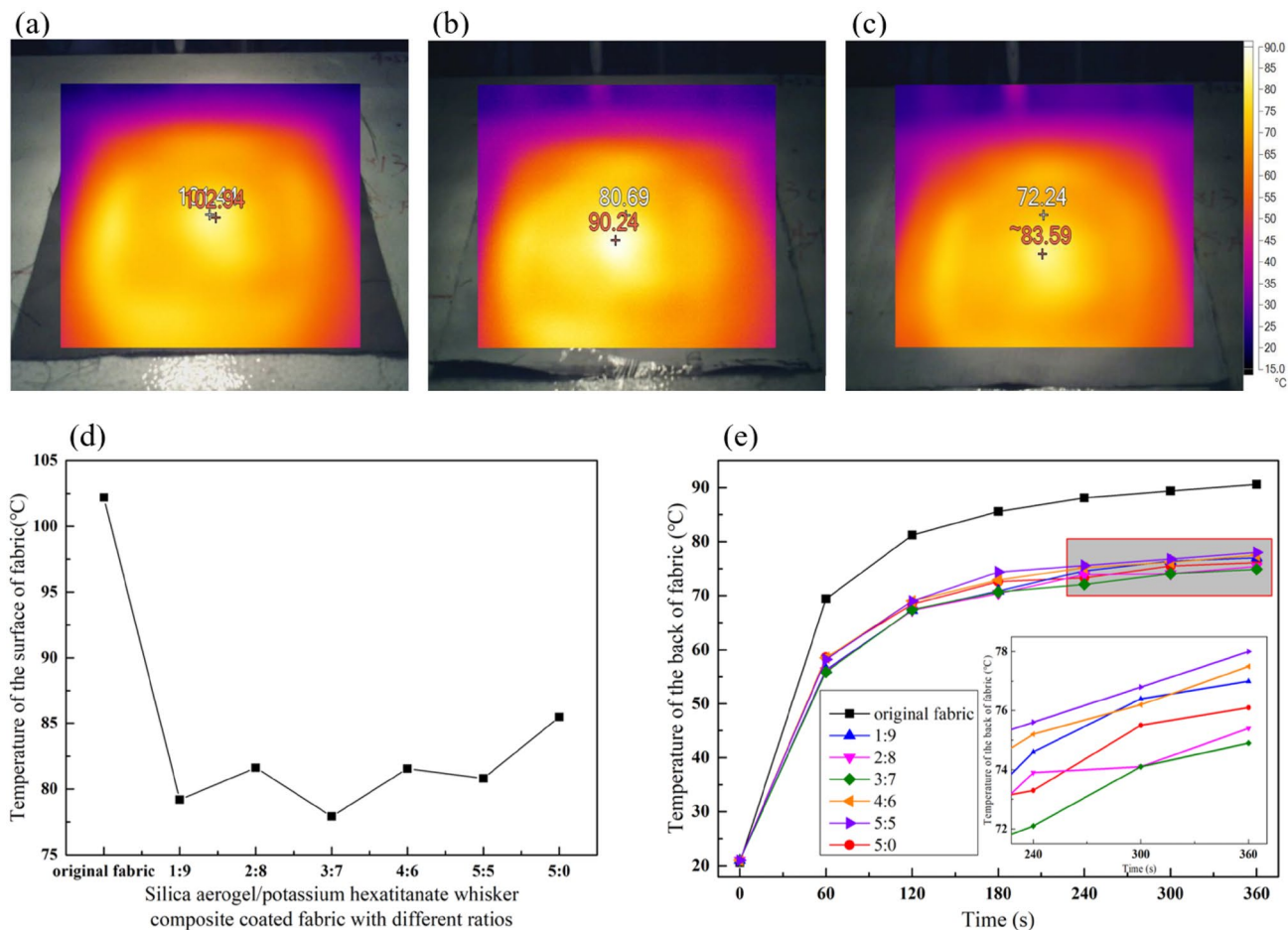


**Fig. 8** Infrared thermal images of **a** the original fabric, **b** the aerogel-coated fabric with a particle ratio of 5:0, and **c** the aerogel/PTW composite coated fabric with a particle ratio of 3:7, **d** was the surface

temperature of each fabric under the heat source tested by the infrared thermal imager, **e** was the temperature rise of the back of each fabric

between the excessive particles in the composite coated fabric, made it difficult for the particles to play their thermal insulation property and thus led to the increase of the thermal conductivity of the composite coated fabric.

### 3.6 Reflectance Spectra of Coated Fabric

In workplaces where molten metal splashes were prone to occur, there were many high-temperature thermal radiations emitted by heating equipment and high-melting liquid metal. Therefore, the surface of the protective fabric needs to have high reflectivity to isolate the thermal radiation containing high energy and to prevent excessive heat builds upon the fabric surface.

The reflectance of the fabrics in 250~2500 nm is shown in Fig. 9. Each composite coated fabric possessed more than 75% reflectivity in the near-infrared band from 750 to 2250 nm where the thermal effect was the highest, which was a significant improvement compared to the original

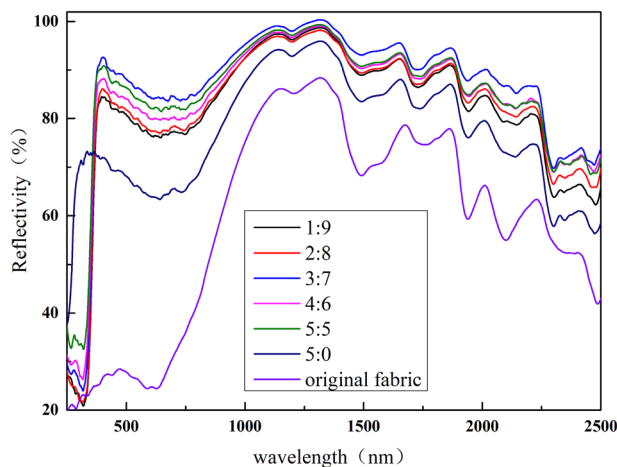


**Fig. 9** Comparison of reflectance spectra of coated fabrics from visible to near-infrared range

fabric. PTW possessed high infrared reflectivity, when the content of PTW increased, the functional particles in the composite coating could increase the probability of interacting with infrared photons, and the scattering and reflection effects were enhanced, so the infrared reflectivity became higher, but too many particles would cause agglomeration and result in the loss of reflectivity. Therefore, as the proportion of PTW in the composite coating increased, the reflectivity of the composite coated fabric first increased and then decreased. When the ratio of aerogel particles to PTW was 3:7, the highest reflectivity of the composite coated fabric was achieved, which was more than 80% in most of the tested wavelength bands, indicating that the PTW as an opacifier made the mixed filler more effective than the single filler. Therefore, the addition of PTW made the composite coated fabric have better heat insulation and reflective properties.

### 3.7 Resistance of the Coated Fabric to Molten Metal Splash

The commercial anti-molten metal splash fabric that contained wool fiber, flame-retardant viscose fiber, para-aramid fiber and a small number of other fibers was purchased for comparison with the coated fabric prepared for this experiment on thermal protection property. The basic physical parameters of the coated fabric prepared in the experiment and commercial anti-molten metal splash fabric are shown in Table 1. According to the results of the previous experiments, the composite coated fabric with a particle ratio of 3:7 and the single aerogel-coated fabric were selected for the aluminum splash resistance test.

Figure 10 shows the damage to the surface of the fabric and the PVC film after pouring 250 g of molten metal. The three tested fabrics were aerogel-coated fabric with a particle ratio of 5:0 and the aerogel/PTW composite coated fabric with a mass ratio of 3:7, and the anti-molten metal splash fabric purchased.

**Table 1** Thickness and weight per square meter of fabrics

Samples (Silica aerogel: PTW)	Weight per square meter ( $\text{g}/\text{m}^2$ )	Thickness (mm)
1:9	354.75	0.625
2:8	347.75	0.612
3:7	343.38	0.601
4:6	340.63	0.603
5:5	335.63	0.598
5:0	329.25	0.595
Original fabric	271.50	0.564
Commercial anti-molten metal splash fabric	307.22	0.587

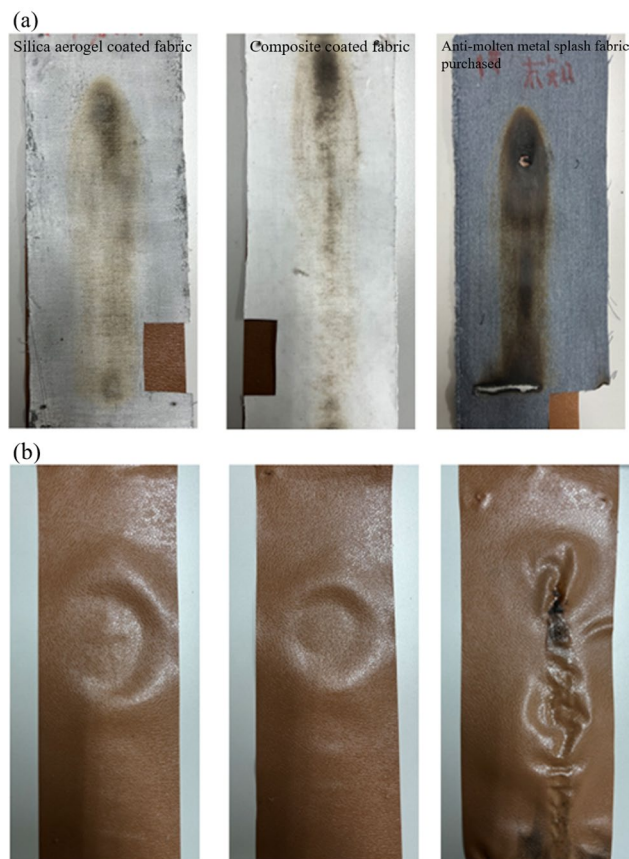


**Fig. 10** After the aluminum splash resistance test, **a** damage to the fabric, **b** damage to the PVC film

As shown in Fig. 10a, after 250 g of metal aluminum liquid pouring, the surface of the three kinds of fabrics appeared to be burned by high-temperature traces, especially obvious in the location of the first contact between aluminum liquid and fabric, which had appeared in varying degrees of charring and blackening phenomenon. The blackening of aerogel-coated fabric and the composite coated fabric did not occur brittle cracking and still had a certain degree of toughness, the degree of charring was slight, no debris generation, the appearance and shape of fabric maintained good, and fabric in the test process did not burn; silica aerogel particles and PTW were low thermal conductivity particles and chemically stable, so they isolated most of the heat when pouring aluminum liquid, which reduced high-temperature damage to the fabric. The thermal insulation coating acted as a protective barrier between the high-temperature aluminum liquid and the fabric. In addition, there was no residual metallic aluminum adhering to the surface for both aerogel-coated fabric and composite coated fabric during the test, which proved that the high-temperature aluminum liquid could slide off cleanly and quickly on the surface of the coated fabric, thus avoiding its long-time exothermic damage to the fabric. The protective fabric purchased had been



completely penetrated by high-temperature aluminum liquid at the pouring point, the fiber and yarn inside the fabric were scorched and broken by high temperature, the charring was serious, and the fabric was found to be completely brittle at the charring after slight grinding by hand, so the fabric had lost its original protective effect, and the fabric had also burned briefly and released a lot of black smoke during the test, which had the possibility of causing secondary damage.

The PVC film (see Fig. 10b) attached to the back of the tested fabric was used to simulate the damage to human skin in the actual use situation. It can be seen that the PVC film attached to the back of the aerogel-coated fabric and the composite coated fabric were not significantly broken, the pattern was clear and the surface was smooth, except in the location of the pouring point due to the longest time of high-temperature impact, which was a slight shrinkage deformation. The purchased fabric was directly penetrated by the high-temperature aluminum liquid, so the surface of PVC film had a charring phenomenon and broken traces caused by aluminum liquid ablation, and the intense heat conduction caused serious shrinkage deformation and distortion of the surface pattern, which proved that the fabric had poor protection effect for molten aluminum.

## 4 Conclusions

Silica aerogel/potassium hexatitanate whisker composite coated fabrics were prepared by using silica aerogel particles and PTW as mixed fillers. The properties of the prepared composite coated fabric were tested and compared with the original fabric and the aerogel-coated fabric. The following conclusions were obtained.

- (1) The structure of PTW was cylindrical form with a relatively large aspect ratio. And the composite coating made silica aerogel particles and PTW doped with each other and evenly bonded to the surface of the fabric, and at the same time, the particles were stacked with each other forming a porous structure. When there were too many aerogel particles, the particles agglomerated into large solids and precipitated out from the coating.
- (2) The XRD pattern of the composite coated fabric showed the presence of diffraction peaks of PTW, and the intensity of the diffraction peaks was proportional to the content of PTW; no crystalline diffraction peaks of silica aerogel were found, indicating that the aerogel used in the experiment was amorphous. The FT-IR spectra showed the structure and composition of the silica aerogel did not change significantly with the increase of the doping amount of PTW.
- (3) When the ratio of silica aerogel to PTW was 3:7, the thermal conductivity of the composite coated fab-

ric was the lowest at 0.232 W/(m·k), which was 19% lower than that of the original fabric and lower than that of the aerogel-coated fabric, proved that the addition of PTW was beneficial to further reduce the thermal conductivity of the coated fabric, and if the proportion of aerogel particles in the composite coating was continued to increase, the thermal conductivity increased instead.

- (4) Under the heat source irradiation, the temperature rise rate and surface temperature of the composite coated fabric were significantly lower than that of the original fabric. When the mass ratio of silica aerogel particles to PTW was 3:7, the temperature rise rate and surface temperature of the composite coated fabric were the lowest, and the surface temperature was 19.35 °C lower than the original fabric.
- (5) The composite coated fabric has more than 75% reflectivity in the band from 750 to 2250 nm. When the ratio of aerogel particles to PTW was 3:7, the composite coated fabric had the highest reflectivity, reaching more than 80% in most of the tested bands.
- (6) The aerogel-coated fabric with a ratio of 5:0 and the composite coated fabric with a mass ratio of 3:7 could withstand the impact of 250 g metal aluminum liquid, with no residual metal adhesion and obvious breakage on the surface of the fabric and no damage to the PVC film.

**Acknowledgements** The authors would like to acknowledge the financial assistance provided by the Key R&D Project of Shandong Province (No.2019JZZY020221) and supported by the Fundamental Research Funds for the Central Universities (No.21D110124/007).

**Data availability statement** The authors confirm that the data supporting the findings of this study are available within the article.

## Declarations

**Conflict of interest** The authors declare no conflicts of interest.

## References

1. H. Mäkinen, *Handb. Fire. Resist. Text* **2**, 581 (2013)
2. B.L. Wei, N. Yang, M.W. Tian, L.J. Qu, S.F. Zhu, *Mater. Lett.* **314**, 131787 (2022)
3. A.K. Maurya, S. Mandal, D.E. Wheeldon, J. Schoeller, M. Schmid, S. Annaheim, M. Camenzind, G. Fortunato, A. Dommann, A. Neels, A. Sadeghpour, R.M. Rossi, *Polymer* **222**, 123634 (2021)
4. Y. Su, J. Yang, R. Li, G. Song, J. Li, *Int. J. Therm. Sci.* **156**, 106501 (2020)
5. M.A. Balkhyour, I. Ahmad, M. Rehan, *Saudi J. Biol. Sci.* **26**, 653 (2019)
6. S.N. Guo, H.F. Wang, C.J. Zhang, P. Zhu, L.F. Li, *Thermochim. Acta.* **704**, 179031 (2021)

7. G.M. Gao, L.N. Miao, G.J. Ji, H.F. Zou, S.C. Gan, *Mater. Lett.* **63**, 2721 (2009)
8. S. Krzemińska, A. Greszta, A. Rózański, M. Safandowska, M. Okrasa, *Microporous. Mesoporous. Mater.* **285**, 43 (2019)
9. B.S.K. Gorle, I. Smirnova, M. Dragan, S. Dragan, W. Arlt, *J. Supercrit. Fluids.* **44**, 78 (2008)
10. J.E. Fesmire, *Cryogenics* **46**, 111 (2006)
11. B. Yuan, S. Ding, D. Wang, G. Wang, H. Li, *Mater. Lett.* **75**, 204 (2012)
12. J. Kuhn, T. Gleissner, M.C. Arduini-Schuster, S. Korder, J. Fricke, *J. Non. Cryst. Solids* **186**, 291 (1995)
13. G.S. Wei, Y.S. Liu, X.X. Zhang, F. Yu, X.Z. Du, *Int. J. Heat Mass Transf.* **54**, 2355 (2011)
14. T.Y. Wei, S.Y. Lu, Y.C. Chang, *J. Phys. Chem. B* **112**, 11881 (2008)
15. S.Q. Zeng, A. Hunt, R. Greif, *J. Non Cryst. Solids* **186**, 271 (1995)
16. J. Yao, X. Gao, Y. Wu, X. Zhao, X. Li, *Ceram. Int.* **43**, 15006 (2022)
17. D. Li, K. Hagos, L. Huang, X. Lu, C. Liu, H.L. Qian, *Ceram. Int.* **43**, 15505 (2017)
18. E. Casamassa, G. Gautier, A. Sin, J. Kukutschova, M.G. Faga, *Open Ceram* **6**, 100128 (2021)
19. P. Ponce-Peña, M. Poisot, A. Rodríguez-Pulido, M.A. González-Lozano, *Materials* **12**, 4132 (2019)
20. J. Hu, J. Ma, W. Deng, *Eur. Polym. J.* **44**, 2695 (2008)
21. J.C. Garay-Jimenez, E. Turos, *Bioorganic Med. Chem. Lett.* **21**, 4589 (2011)
22. S.M. Shang, Y.X. Wang, K-L. Chiu, S.X. Jiang, *Compos. B. Eng.* **177**, 107408 (2019)

Springer Nature or its licensor (e.g. a society or other partner) holds exclusive rights to this article under a publishing agreement with the author(s) or other rightsholder(s); author self-archiving of the accepted manuscript version of this article is solely governed by the terms of such publishing agreement and applicable law.